Statistics of geomagnetic storms and ionospheric storms at low and mid latitudes in two solar cycles

D. Vijaya Lekshmi,[1] N. Balan,[2] S. Tulasi Ram,[3] and J. Y. Liu[2]

Received 29 July 2011; revised 24 August 2011; accepted 13 September 2011; published 29 November 2011.

[1] The statistics of occurrence of the geomagnetic storms, and ionospheric storms at Kokubunji (35.7°N, 139.5°E; 26.8°N magnetic latitude) in Japan and Boulder (40.0°N, 254.7°E; 47.4°N) in America are presented using the Dst and peak electron density (Nmax) data in 1985–2005 covering two solar cycles (22–23) when 584 geomagnetic storms (Dst ≤ −50 nT) occurred. In addition to the known solar cycle and seasonal dependence of the storms, the statistics reveal some new aspects. (1) The geomagnetic storms show a preference for main phase (MP) onset at around UT midnight especially for major storms (Dst ≤ −100 nT), over 100% excess MP onsets at UT midnight compared to a uniform distribution. (2) The number of positive ionospheric storms at Kokubunji (about 250) is more than double that at Boulder, and (3) the occurrence of the positive storms at both stations shows a preference for the morning-noon onset of the geomagnetic storms as expected from a physical mechanism of the positive storms. (4) The occurrence of negative ionospheric storms at both stations follows the solar cycle phases (most frequent at solar maximum) better than the occurrence of positive storms, which agrees with the mechanism of the negative storms.

Citation: Vijaya Lekshmi, D., N. Balan, S. Tulasi Ram, and J. Y. Liu (2011), Statistics of geomagnetic storms and ionospheric storms at low and mid latitudes in two solar cycles, *J. Geophys. Res.*, *116*, A11328, doi:10.1029/2011JA017042.

1. Introduction

[2] A series of rapid changes takes place in the global thermosphere and ionosphere following the onset of geomagnetic storms. (1) High latitude thermosphere gets heated and expands, which causes equatorward neutral winds, surges and TADs (traveling atmospheric disturbances) [e.g., *Prölss and Jung*, 1978; *Roble et al.*, 1982], which all together change the thermospheric composition [e.g., *Mayr and Volland*, 1973]. (2) High latitude ionospheric electric fields penetrate to low latitudes [e.g., *Rastogi*, 1977]. (3) Subauroral electric fields intensify and expand equatorward [e.g., *Foster*, 1993]. (4) Disturbance dynamo electric fields develop [e.g., *Blanc and Richmond*, 1980]. (5) The changes in the thermosphere and ionospheric electric fields produce rapid and sometimes dramatic changes in the ionospheric density [e.g., *Matsushita*, 1959; *Mannucci et al.*, 2005], which are called ionospheric storms.

[3] The ionospheric electron density (Ne), peak electron density (Nmax) and total electron content (TEC) often increase/decrease very much from their average quiet time levels, which are known as positive/negative ionospheric storms. The ionospheric storms are studied for over 50 years [e.g., *Matsushita*, 1959; *Jones and Rishbeth*, 1971]. Excellent review articles are presented by *Obayashi* [1964], *Matuura* [1972], *Prölss* [1995], *Buonsanto* [1999], and *Mendillo* [2006]. Good case studies of the spacial coverage of the ionospheric storms are also presented in several papers [e.g., *Essex et al.*, 1981; *Mannucci et al.*, 2005]. The statistics of the ionospheric storms are also reported. For example, *Balan and Rao* [1990] reported the dependence of the ionospheric response at low and mid latitudes on the local time of onset and intensity of the geomagnetic storms using the TEC and Nmax data during 60 geomagnetic storms in 1968–72. *Mendillo and Narvaez* [2009, 2010] reported detailed studies of the ionospheric storms at geophysically equivalent subauroral sites having comparable geographic and geomagnetic latitudes using the Nmax data for the 206 geomagnetic storms in solar cycle 20 (1964–1976). Modeling studies have also been carried out to reproduce ionospheric storms and understand their physical mechanisms [i.e., *Richmond and Matsushita*, 1975; *Fuller-Rowell et al.*, 1994; *Burns et al.*, 1995; *Lin et al.*, 2005; *Vijaya Lekshmi et al.*, 2007; *Lu et al.*, 2008].

[4] From these studies it is known that the nature of the ionospheric storms (positive or negative) depends on local time, season and latitude. At low and mid latitudes, geomagnetic storms with nighttime main phases (MPs) in all seasons generally produce negative ionospheric storms. The storms with daytime (especially morning-noon) MPs in winter and equinox in general produce positive ionospheric storms and those in summer produce positive followed by negative ionospheric storms. There are also large variations from these general patterns [e.g., *Balan and Rao*, 1990; *Prölss*, 1995; *Mendillo*, 2006]. The tilt of the geomagnetic

[1]Department of Physics, University of Kerala, Trivandrum, India.
[2]Institute of Space Science, National Central University, Chung-Li, Taiwan.
[3]RISH, Kyoto University, Kyoto, Japan.

0148-0227/11/2011JA017042

Table 1. Geomagnetic Storms

	Number
Moderate (−100 nT < Dst < −50 nT)	409
Major (−250 nT < Dst < −100 nT)	153
Super (Dst < −250 nT)	22
Total (Dst < −50 nT)	584

and geographic equators introduces significant differences in the ionospheric storms even in nearly conjugate locations [e.g., *Mendillo and Narvaez*, 2009, 2010]. The ionospheric storms at equatorial latitudes are in general opposite to those at higher latitudes [e.g., *Sastri et al.*, 2000; *Tulasi Ram et al.*, 2009; *Sreeja et al.*, 2009; *Huang et al.*, 2010a].

[5] It is also understood that the ionospheric storms are produced by the rapid modifications of the known ionospheric processes. The negative ionospheric storms at low and mid latitudes arise mainly from the thermospheric composition changes that make the thermosphere richer in molecular concentration [N_2] and poorer in atomic concentration [O] so that chemical recombination becomes faster than normal [e.g., *Prölss*, 1995; *Fuller-Rowell et al.*, 1994]. The positive ionospheric storms at low and mid latitudes involve mainly the rapid slow-down of both the recombination processes and downward diffusion of plasma by the mechanical effects of storm-time equatorward neutral winds [*Prölss and Jung*, 1978; *Balan et al.*, 2010, 2011a], and rapid strengthening of the equatorial plasma fountain by enhanced eastward prompt penetration electric fields (PPEFs) [e.g., *Kikuchi et al.*, 1978; *Kelley et al.*, 2004; *Mannucci et al.*, 2005; *Balan et al.*, 2009]. The positive storms at high-mid latitudes involve the intensification and equatorward expansion of the sub-auroral electric fields [*Foster*, 1993; *Heelis et al.*, 2009]. At equatorial latitudes, the eastward PPEFs during the MPs have effects which are opposite to those at higher latitudes [e.g., *Batista et al.*, 1991; *Balan et al.*, 2011b].

[6] According to a physical mechanism of the positive ionospheric storms at low and mid latitudes [*Balan et al.*, 2010, 2011a], the positive storms are expected to occur frequently at ±20° to ±30° magnetic latitudes and during the morning-noon onset of geomagnetic storms. To check these predictions statistically, we analyze the ionospheric storms at a low-mid latitude station Kokubunji (26.8°N magnetic latitude) and a mid latitude station Boulder (47.4°N magnetic latitude) using the peak electron density (Nmax) data in 21 years (1985–2005) covering two solar cycles (22–23). 584 geomagnetic storms occurred during the 21 year period. In addition to supporting the predictions, the statistics presented below bring out a few more new aspects of geomagnetic and ionospheric storms.

[7] The physical mechanism of the positive ionospheric storms referred above [e.g., *Balan et al.*, 2010, 2011a] involves eastward PPEF and equatorward neutral winds (and surges). However, the eastward PPEF alone is unlikely to produce the positive storms at low and mid latitudes because the resulting $\mathbf{E} \times \mathbf{B}$ drift (1) cannot raise the ionosphere to high altitudes of reduced chemical loss (due to lack of support) and (2) accelerates the downward diffusion of plasma along the geomagnetic field lines to low altitudes of high chemical loss. On the other hand, the neutral winds alone can produce the positive storms centered at around ±16° magnetic latitudes by raising and supporting the ionosphere at high altitudes and reducing the downward diffusion of plasma. The winds and eastward PPEF together also produce the positive storms but centered at around ±20° to ±30° magnetic latitudes due the PPEF shifting the EIA crests to higher than normal latitudes. In this case the positive storms are narrow in latitudes, and sharp in density at the point of convergence of plasma due to the forward fountain and equatorward winds.

2. Data and Analysis

[8] The hourly values of the geomagnetic activity index (Dst) is obtained from the World Data Centre in Kyoto (http://swclob-kugi.kyoto-u.ac.jp). As listed in Table 1 a total of 584 geomagnetic storms with minimum Dst ≤ −50 nT occurred in 1985–2005, which include 409 moderate storms (−100 ≤ Dst < −50 nT), 153 major storms (−250 ≤ Dst < −100 nT) and 22 super storms (Dst ≤ −250 nT). The hourly values of the ionospheric critical frequency f_oF_2 at Kokubunji(35.7°N, 139.5°E; 26.8°N magnetic latitude) in Japan and Boulder (40.0°N, 254.7°E; 47.4°N magnetic latitude) in America are taken from the SPIDR site (http://spidr.ngdc.noaa.gov/spidr). Though 584 geomagnetic storms occurred in 1985–2005, the ionospheric data are available only for 524 storms at Kokubunji and 485 storms at Boulder; no data at Boulder in 2003.

[9] The critical frequency is converted to the peak electron density Nmax (=$1.24 \times f_oF_2^2 \times 10^4$ cm^{-3} with f_oF_2 in MHz). The storm time deviation of Nmax (ΔNmax) for 72 hours following the onset of each geomagnetic storm is obtained on an hourly basis by subtracting the seven quiet-day average hourly values prior to the storm from the corresponding hourly values during the storm. If two geomagnetic storms fall within ten days of each other, the quiet-day average values prior to the first storm are used for both storm periods. A geomagnetic storm is considered to produce an ionospheric storm if ΔNmax exceeds ±25% for more than three hours; ±25% is set to represent the day-to-day variability of the ionosphere under quiet conditions; furious changes in the data that sometimes occur are removed by visually examining the Nmax variations. The maximum positive value of ΔNmax (for positive storms) and maximum negative value of ΔNmax (for negative storms) are noted, which are taken to represent the strength of ionospheric storms.

3. Geomagnetic Storms

[10] Figure 1a shows the distribution of occurrence and intensity (minimum Dst) of the geomagnetic storms as function of days in 1985–2005 (Figure 1a, top), which is compared with the monthly mean solar activity index (F10.7) in Figure 1a (bottom). Figure 1b shows the number of occurrence of the storms as function of year (or solar cycle phases), months of year, and universal time (UT) of main phase (MP) onset. The MP onset is taken as the UT hour when Dst starts to decrease. As shown in Figures 1a and 1b, the occurrence and intensity of the storms follow the known solar activity dependence, more frequent and more intense at solar maximum than at solar minimum. However, intense storms sometimes occur frequently in the

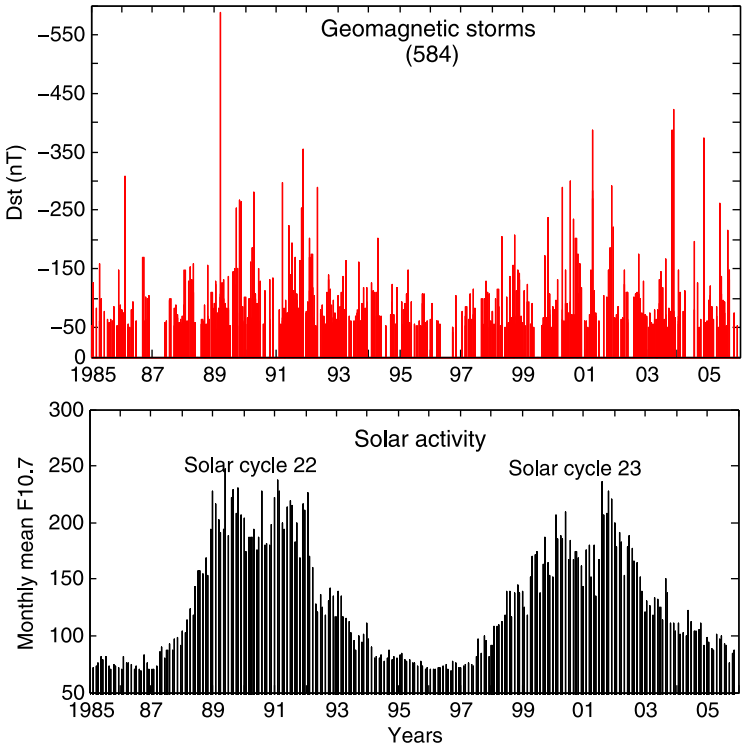

Figure 1a. (top) Occurrence and intensity (Dst ≤ −50 nT) of the geomagnetic storms as a function of days in 1985–2005 and (bottom) corresponding monthly mean solar activity index F10.7 (the lines look different due to compression).

descending phases of solar cycles, for example in 2003–04. With months of the year (Figure 1b), the storms show the known more frequent occurrence at equinoxes than in solstices (Figure 1b, middle), discussed in section 5. However, with time of the day, the MP onset of the storms reveals significant preferences at around UT midnight (00 UT) and midday (12 UT). This new aspect is studied separately for major and super storms (Dst ≤ −100 nT) in section 4.3.

4. Ionospheric Storms

[11] The ionospheric storms are classified into five groups based on the variation of ΔNmax. The storms are classified as positive storms (P-storms) or negative storms (N-storms) depending on whether ΔNmax is positive or negative following the onset of geomagnetic storms (small fluctuations of less than ±25% are neglected). Some ionospheric storms show initial positive ΔNmax (>25% for more than three hours) followed by negative ΔNmax, which are classified as PN-storms. A small number of storms are found to have initial negative ΔNmax followed by positive ΔNmax; they are classified as NP-storms. There are also non-significant ionospheric storms (NS-storms) for which ΔNmax is weak (less than ±25%). Examples of the ionospheric storms are shown in Figures 2a–4c. In the examples, the storm-time Nmax is compared with the seven quiet-day average Nmax. The hourly standard deviations of the quiet-day averages are not shown for simplicity.

[12] Figures 2a and 2b show examples of the positive ionospheric storms (P-storms) at Kokubunji and Boulder; they correspond to the geomagnetic storms in October 1999 and February 1989 with MP onsets at 09 LT and 07 LT respectively. The positive storms as shown by the statistics in the next section correspond mainly to the morning-noon MP onsets. The geomagnetic storms with nighttime MP onsets in general are found to produce negative ionospheric storms as shown by the examples in Figures 3a and 3b. These examples correspond to the geomagnetic storms in October 1991 and November 2001 with MP onsets at 04 LT and 00 LT respectively. However, the geomagnetic storms with daytime MP onsets in summer in general produce positive storms followed by negative ones (PN-storms) as shown by an example in Figure 4a, which corresponds to a geomagnetic storm in June 1991 with MP onset at 11 LT in Boulder; the positive phase lasts until sunset, which is followed by a large negative phase. There are also a small number of storms having initial negative phase followed by positive phase (NP-storms) as shown by an example in Figure 4b, which corresponds to a geomagnetic storm with MP onset at 00 LT in Boulder. Figure 4c shows an example of a non-significant ionospheric storm (NS-storm). The ionosphere over Kokubunji remains unaffected during the geomagnetic storm in November 1989. Examples of PN-, NP- and NS-storms are shown for one of the stations for simplicity.

[13] Tables 2 and 3 list the number of different types of ionospheric storms at Kokubunji (26.8°N magnetic latitude) and Boulder (47.4°N magnetic latitude). As listed, the number of positive storms at Kokubunji (255) is more than double that at Boulder (123). On the other hand the number

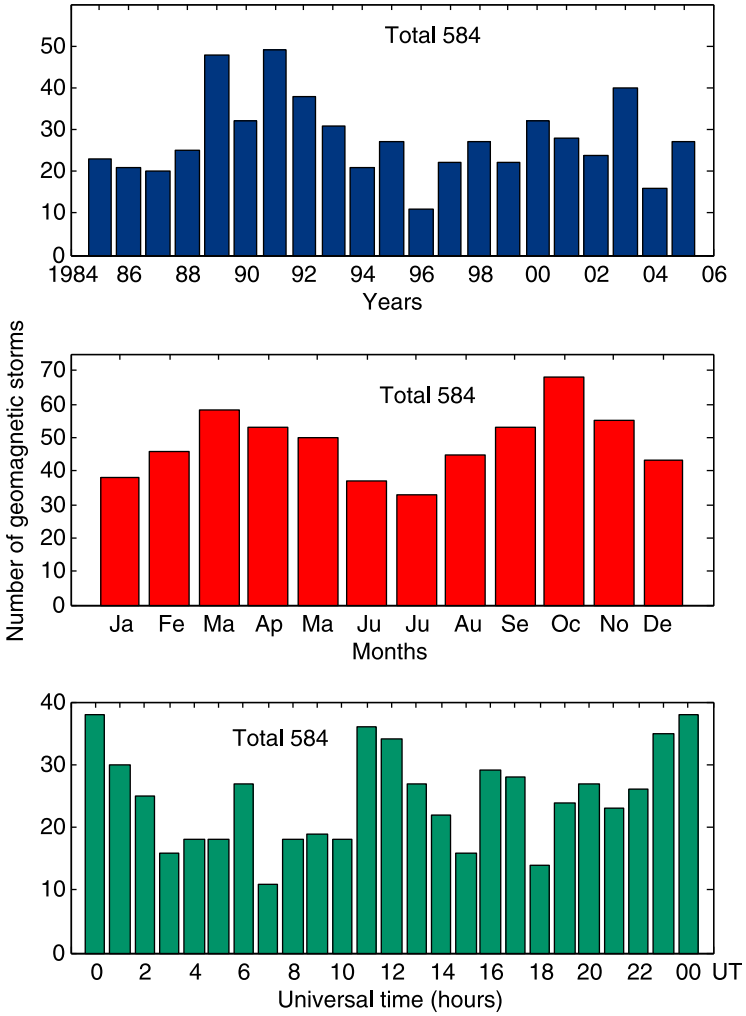

Figure 1b. Number of main phase onset of geomagnetic storms (Dst ≤ −50 nT) in 1985–2005 as functions of (top) years, (middle) months of year, and (bottom) universal time of day.

of negative storms at Kokubunji is half of that at Boulder, 103 against 224. There are also a significant number of PN-storms at both locations, which are also more at Kokubunji (62) than at Bounder (52).However, the NP-storms are small in number at both locations, less at Kokubunji (12) than at Boulder (17). These statistics of the ionospheric storms seems to agree with the expected preferential location (±20° to ±30° magnetic latitudes) for the frequent occurrence of positive storms, discussed in section 5. There are also a considerable number of NS-storms (non-significant storms) at both locations (92 at Kokubunji and 69 at Boulder).

4.1. Solar Activity Dependence

[14] Figures 5a and 5e show the yearly distribution of the number of geomagnetic storms for which ionospheric data are available at Kokubunji (524) and Boulder (485); the panels below show the corresponding distribution of the different types of ionospheric storms at the two stations. The occurrence of the geomagnetic storms again follows the solar cycle phases, most frequent at solar maximum. The occurrence of the ionospheric storms in general depends both on solar cycle phases and year-by-year distribution of the geomagnetic storms. However, the occurrence of the negative storms (Figures 5c and 5g) follows the solar cycle phases (most frequent at solar maximum) better than the occurrence of the positive storms (Figures 5b and 5f) at both stations, which is discussed in section 5. The distribution of non-significant ionospheric storms (Figures 5d and 5h) is similar to that of the geomagnetic storms (Figures 5a and 5e).

4.2. Seasonal Dependence

[15] The monthly distribution of the number of storms is shown in Figures 6a and 6e for geomagnetic storms and the panels below for the different types of ionospheric storms (left for Kokubunji and right for Boulder). As shown, the occurrence of the ionospheric storms follows the seasons rather than the distribution of the geomagnetic storms. Irrespective of the location of preference, positive storms (Figures 6b and 6f, red histograms) occur frequently in winter and equinoxes (September through April), and negative storms (Figures 6c and 6g, red histograms) occur mainly in summer (May-August) at both stations. However,

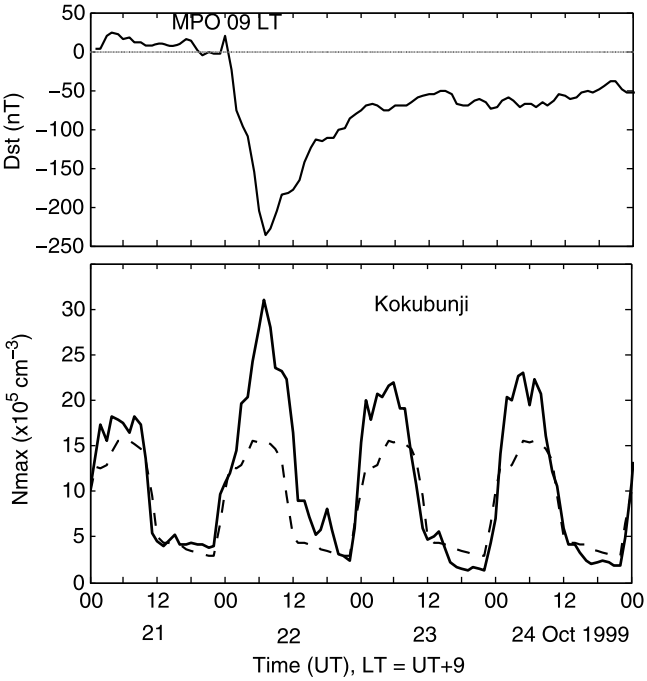

Figure 2a. (bottom) Example of a positive ionospheric storm at Kokubunji during (top) the geomagnetic storm of 22–25 October 1999. Following the main phase onset (MPO) at around 09 LT (=UT + 9 hrs) on 22 October the storm-time Nmax (solid curve) remains much greater than the seven quiet-day average prior to the storm (dashed curve).

at Boulder where the negative storms are most frequent, they occur at equinoxes and in winter also (Figure 6g, red histograms). The occurrence of the PN-storms (Figures 6b and 6f, green histograms) is also frequent in summer at both stations. The seasonal dependence of the ionospheric storms agrees with earlier studies [e.g., *Prölss*, 1995; *Mendillo and Narvaez*, 2009, 2010]. The NS-storms (Figures 6d and 6h), however, follow the distribution of the geomagnetic storms rather than seasons as expected.

4.3. Local Time Dependence

[16] Local time distribution of the ionospheric storms is studied for all geomagnetic storms (Dst ≤ −50 nT) together and for major and supper storms (Dst ≤ −100 nT) separately. Though there are 175 major and super storms (Table 1), the ionospheric data at both stations are available only for 155 storms. Figures 7a and 7c show the local time distribution of the MP onset of the major and super storms (together) for which ionospheric data are available; Figures 7b and 7d show the corresponding distributions of the positive and negative ionospheric storms; P-storms and PN-storms together are considered as positive storms, and N-storms and NP-storms together as negative storms. The positive and negative ionospheric storms do not add up to the geomagnetic storms (Figure 7) because the non-significant ionospheric storms (16 at Kokubunji and 18 at Boulder) are not considered. Considering all geomagnetic storms (Dst ≤ −50 nT) together, Table 2 lists the number of different types of ionospheric storms for morning-noon (05–12 LT) MP onset, noon-evening (13–19 LT) MP onset and nighttime (20–04 LT) MP onset at Kokubunji. Table 3 gives a similar list for Boulder.

[17] As shown by Figures 7a and 7c the MP onset of the major and super geomagnetic storms shows clear peaks at around 09 LT at Kokubunji and 16 LT at Boulder, which correspond to UT midnight. The UT midnight preference (about 130% and 100% excess MP onsets compared to a uniform distribution, Figure 7) seems to be significant, discussed in section 5. However, a secondary preference at around UT midday when all storms are considered together (Figure 1b) disappears when major and super storms alone are considered (Figure 7).

[18] As listed in Tables 2 and 3 and shown in Figures 5–7, irrespective of the intensity of the geomagnetic storms, the number of positive ionospheric storms at Kokubunji is more than double that at Boulder. Also, irrespective of the location of preference, the positive storms at both stations occur most frequently for the morning-noon (05–12 LT) MP onsets with clear peaks for the MP onsets at around 09–10 LT (Figures 7b and 7d, red histograms). The local time preference does not seem to be due to the distribution of the MP onsets (Figures 7a and 7c) because the preference is similar at both stations. However, the preference is most clear at Kokubunji where the UT midnight preference for the MP onset (Figure 7a) corresponds to 09 LT. The number of negative storms (Figures 7b and 7d, blue histograms) are also less in the morning-noon sector and more in the nighttime sector at both stations.

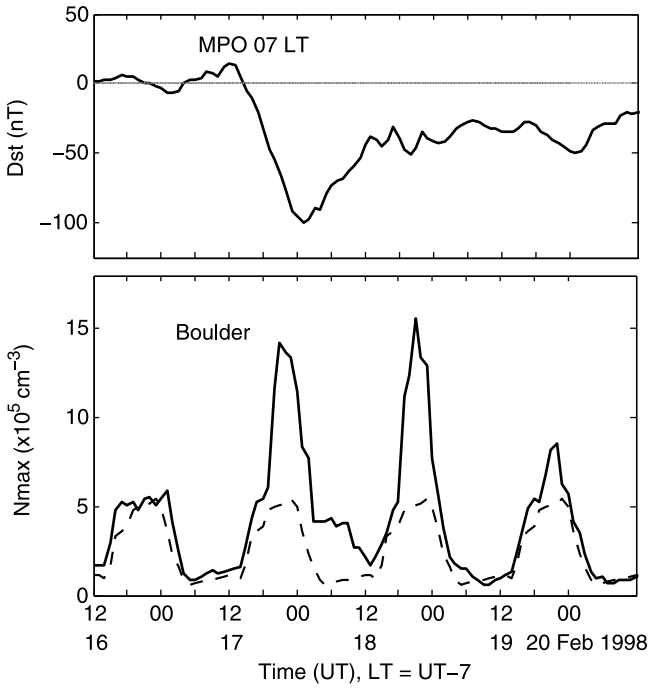

Figure 2b. (bottom) Example of a positive ionospheric storm at Boulder during (top) the geomagnetic storm of 17–20 February 1998. Following the main phase onset (MPO) at around 07 LT (=UT-7 hrs) on 17 February the storm-time Nmax (solid curve) remains much greater than the seven quiet-day average prior to the storm (dashed curve).

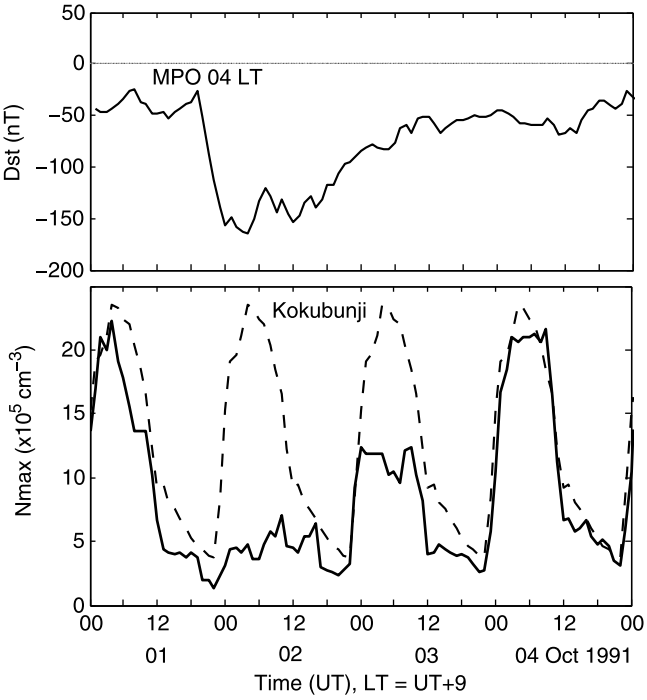

Figure 3a. (bottom) Example of a negative ionospheric storm at Kokubunji during (top) the geomagnetic storm of 2–4 October 1991. Following the main phase onset (MPO) at around 04 LT (=UT+9 hrs) on 2 October the storm-time Nmax (solid curve) remains much lower than the seven quiet-day average prior to the storm (dashed curve).

4.4. Strength of Ionospheric Storms

[19] As mentioned in section 2, the maximum positive value of ΔNmax (for positive storms) and maximum negative value of ΔNmax (for negative storms) are taken to represent the strength of the ionospheric storms. PN-storms and NP-storms are not considered because they have both positive and negative phases. Minimum Dst and integrated Kp during MP are considered to represent the intensity of the geomagnetic storms. Figure 8 shows the dependence of the magnitude of maximum ΔNmax on minimum Dst separately for the positive and negative storms at Kokubunji and Boulder; all geomagnetic storms (Dst ≤ −50 nT) are considered. The main feature of Figure 8 is small positive correlations and large scatter. The correlation is also better for the negative storms at the higher latitude station Boulder. The correlations between ΔNmax and integrated Kp (not shown) are also found to be similar to those in Figure 8. The small correlation and large scatter suggest that the strength of the ionospheric storms depends not only on the intensity of geomagnetic storms but also on a number of other parameters, discussed in section 5.

5. Discussion

[20] The main points of the statistics of occurrence of the geomagnetic storms, and ionospheric storms at Kokubunji (26.8°N magnetic latitudes) and Boulder (47.4°N magnetic latitudes) obtained by analyzing the Dst and Nmax data in two solar cycles (1985–2005) when 584 geomagnetic storms occurred are listed and briefly discussed.

[21] 1. The geomagnetic storms reveal a preference for main phase (MP) onset at around UT midnight, especially for major storms (Figure 7). The UT midnight preference (over 100% excess MP onsets compared to a uniform distribution) is as significant as the equinoctial preference and is found to be consistent in all solar cycles (result not shown). Though the preference is not understood, it is noted that the corresponding noon meridian is in the Pacific sector where the separation between geomagnetic and geographic equators is a minimum (nearly zero) and declination angle is nearly constant so that magnetosphere and ring current become symmetric in north and south. That may help efficient solar wind-magnetosphere coupling and ring current intensification, which may cause the frequent occurrence of MP onset. The geomagnetic storms are also frequent at equinoxes compared to solstices, for which several explanations have been proposed [e.g., *Russell and McPherron*, 1973; *Newell et al.*, 2001, and references therein]. The *Russell and McPherron* [1973] explanation is based on the 26° angle between the equatorial plans of Sun and Earth and 11° tilt of Earth dipole axis. However, *Newell et al.* [2001] suggest that geomagnetic activity can also maximize when the night side auroral oval in both hemispheres is in darkness, which happens at around equinoxes. The occurrence and intensity of the geomagnetic storms also exhibit the well known solar cycle dependence, most frequent and intense at

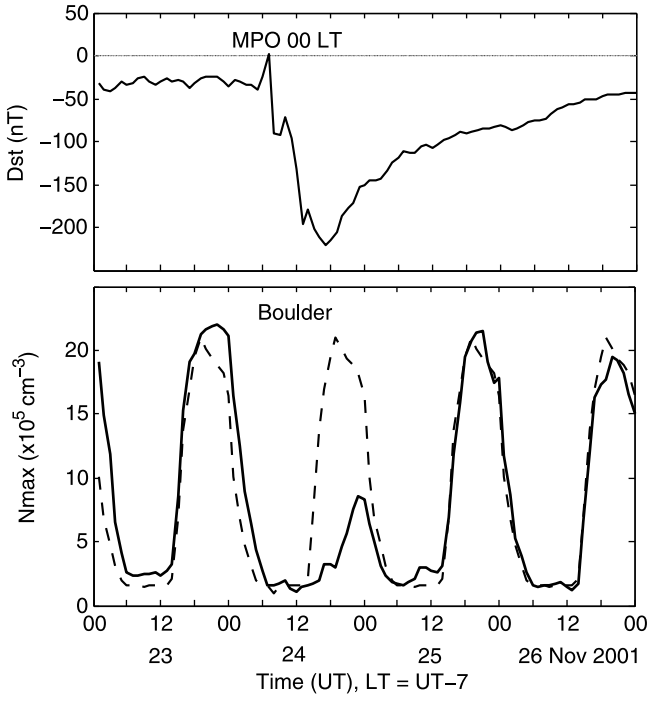

Figure 3b. (bottom) Example of a negative ionospheric storm at Boulder during (top) the geomagnetic storm of 24–26 November 2001. Following the main phase onset (MPO) at around 00 LT (=UT-7 hrs) on 24 November 2001 the storm-time Nmax (solid curve) remains much lower than the seven quiet-day average prior to the storm (dashed curve).

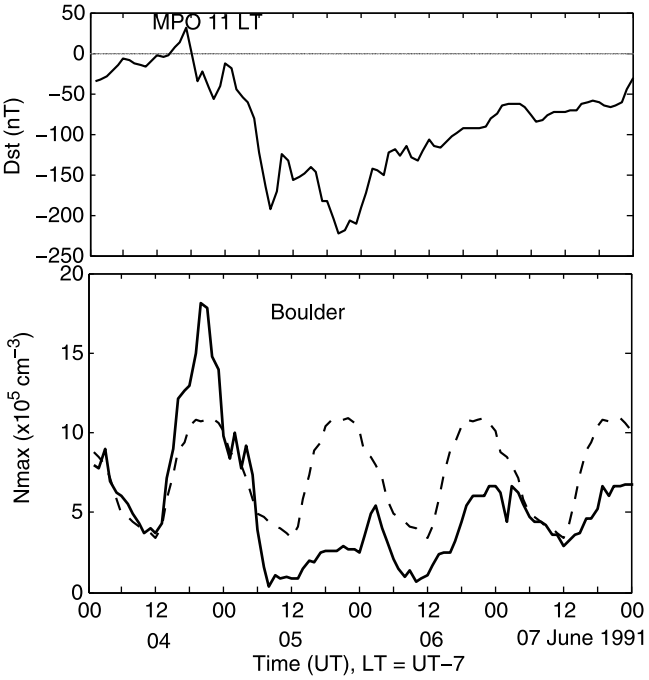

Figure 4a. (bottom) Example of a positive followed by negative ionospheric storm at Boulder during (top) the geomagnetic storm of 04–07 June 1991. Following the main phase onset (MPO) at 11 LT (=UT-7 hrs) the storm-time Nmax (solid curve) remains greater than the seven quiet-day average prior to the storm (dashed curve) until sunset, which is followed by a large decrease.

solar maximum, though sometimes intense storms occur frequently at the declining phases of solar cycles, for example in 2003–04, as reported by *Gonzalez et al.* [1994].

[22] 2. The number of positive ionospheric storms (Tables 2 and 3, Figures 5–7) at Kokubunji (26.8°N magnetic latitudes) is more than double that at Boulder (47.4°N magnetic latitudes). According to a mechanism of the positive storms [*Balan et al.*, 2010, 2011a], the storms can occur either due to the mechanical effects of storm-time equatorward neutral winds and surges alone or together with daytime eastward PPEFs. In the latter case, considering the variability of the winds and PPEFs, the strength of the positive storms (described in section 1) is centered at ±20° to ±30° magnetic latitudes. The high latitude thermospheric neutral winds, temperatures and composition have been measured using ground-based and satellite techniques and compared with models [e.g., *Rees et al.*, 1980; *Shepherd et al.*, 1993; *Prölss*, 1995; *Reigber et al.*, 2002]. Recent observations show that the heating and expansion of the ionosphere (and hence thermosphere) during geomagnetic storms begin with the onset of the initial phase of the storms [e.g., *Balan et al.*, 2008]. The resulting winds are found to reach the equator during all geomagnetic storms [*Lei et al.*, 2010; *Balan et al.*, 2011a], preceded by fast surges during storms with short and steady MPs [e.g., *Fuller-Rowell et al.*, 1994; *Balan et al.*, 2011a]. The eastward PPEFs also occur during part or whole of the MP of all geomagnetic storms [e.g., *Huang et al.*, 2010a; *Balan et al.*, 2011b]. The positive ionospheric storms are therefore expected more frequently at ±20° to ±30° magnetic latitudes than at other latitudes as observed. The variability of quiet time **E** × **B** drift, neutral winds and separation between geomagnetic and geographic equators can cause variations in the latitude for the most probable occurrence of the positive storms. However, the strength of the positive storms (deviation from quiet time levels) is found to be strong within ±20° to ±30° magnetic latitudes in all longitudes during major geomagnetic storms [*Mannucci et al.*, 2005; *Lei et al.*, 2010; *Balan et al.*, 2010, 2011a, and references therein]. The present statistics suggests that it may be true for moderate storms also. The positive storms at sub-auroral latitudes, however, can maximize due to intensified sub-auroral electric fields, without contributions from the strengthening of eastward PPEFs [e.g., *Heelis et al.*, 2009].

[23] 3. Irrespective of the intensity of the geomagnetic storms and location, positive ionospheric storms occur frequently in the morning-noon local time sector of MP onset (Tables 2 and 3, Figure 5). This is expected because the positive storms involve the daytime production of ionization [e.g., *Kelley et al.*, 2004; *Balan et al.*, 2010], which dominates over the chemical loss of ionization in the morning-noon local time sector.

[24] 4. The occurrence of negative ionospheric storms follows the solar cycle phases (most frequent at solar maximum) better than the occurrence of positive ionospheric storms (Figure 5). This can be understood from the

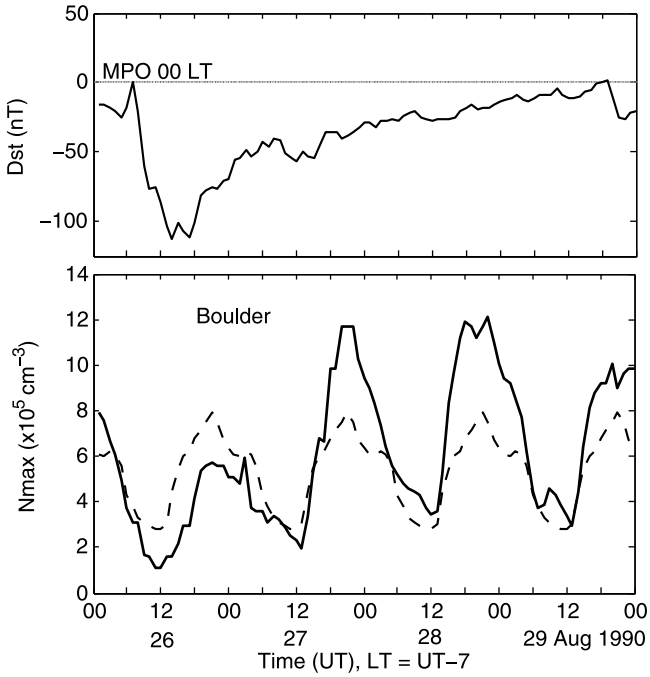

Figure 4b. (bottom) Example of a negative followed by positive ionospheric storm at Boulder during (top) the geomagnetic storm of 26–29 August 1990. Following the main phase onset (MPO) at 00 LT (=UT-7 hrs) on 26 August the storm-time Nmax (solid curve) remains lower than the seven quiet-day average prior to the storm (dashed curve) for nearly a day, which is followed by large increases.

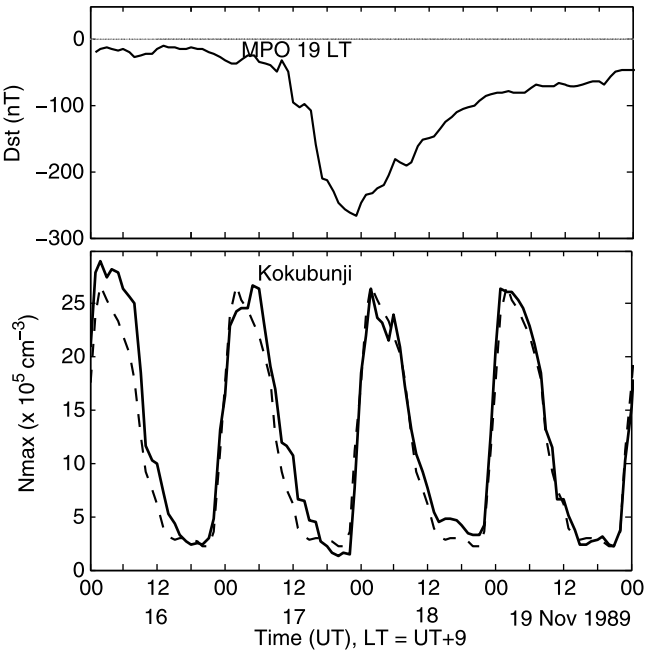

Figure 4c. (bottom) Example of a non-significant ionospheric storm at Kokubunji during (top) the geomagnetic storm of 17–20 November 1989. The storm-time Nmax (solid curve) remains almost the same as the seven quiet-day average prior to the storm (dashed curve).

mechanism of the negative storms [e.g., *Fuller-Rowell et al.*, 1994; *Prölss*, 1995], described in section 1. Due to thermal expansion, the quiet time $[O]/[N_2]$ ratio at all pressure (and height) levels is smaller at solar maximum than at solar minimum. In such a background thermosphere, the chemical effects of the storm-time neutral winds can easily make the $[O]/[N_2]$ ratio much smaller at solar maximum than at solar minimum. In other words, negative ionospheric storms can occur easily at solar maximum than at solar minimum.

[25] 5. Irrespective of location the negative ionospheric storms are frequent in summer months (Figure 6), which also agrees with the mechanism of the negative storms [e.g., *Prölss*, 1995]. The quiet time summer to winter thermospheric circulation makes the background $[O]/[N_2]$ ratio smaller in summer than in winter (and equinox) at all pressure (and height) levels. The chemical effects of storm-time neutral winds can therefore produce negative ionospheric storms easily in summer.

[26] 6. The strength of both positive and negative ionospheric storms has a small positive correlation and large scatter with the intensity of the geomagnetic storms (Figure 8). This indicates the large variability of the drivers of the ionospheric storms. As mentioned in section 1, the drivers include the heating and expansion of high latitude thermosphere and resulting equatorward neutral surges and winds [e.g., *Prölss and Jung*, 1978; *Roble et al.*, 1982] that change thermospheric composition [*Mayr and Volland*, 1973; *Fuller-Rowell et al.*, 1994] and also exert mechanical and electrical effects (disturbance dynamo) on the ionosphere [e.g., *Blanc and Richmond*, 1980;*Prölss and Jung*, 1978; *Balan et al.*, 2010, 2011a]. The penetration of high latitude electric fields to low latitudes [e.g., *Sastri*, 2002; *Fejer et al.*, 2007; *Abdu et al.*, 2008;*Huang et al.*, 2010b] and intensification and equatorward expansion of sub-auroral electric fields [e.g., *Foster*, 1993] also play major roles in the generation of ionospheric storms [e.g., *Kelley et al.*, 2004; *Heelis et al.*, 2009]. The strength of these coupled drivers depends on the intensity (e.g., minimum Dst) of the geomagnetic storms, and on the background thermosphere and ionosphere (or on time of the day, season, level of solar activity and location). The coupled drivers and background thermosphere and ionosphere together generate positive or negative ionospheric storms, and control their strengths in complicated ways which is not understood. The positive and negative storms could also merge in some locations reducing their strengths. It is also known that short and steady MPs (though weak) can cause strong thermospheric and ionospheric storms compared to long and fluctuating MPs (though intense) through impulsive response [e.g., *Balan et al.*, 2011a].

[27] 7. In addition to the positive and negative ionospheric storms, the statistics (Tables 2 and 3, Figure 6) shows a significant number of positive storms followed by negative ones (PN-storms), which occur mainly in summer months. There are also a small number of negative storms followed by positive ones (NP-storms), the negative phase of which usually correspond to nighttime MP onset and positive phase correspond to the daytime re-intensification of the storm during the RP of the main storm. There are also a significant number of non-significant ionospheric storms (NS-storms), which seems to suggest the longitude dependencies of penetration electric fields and energy input at high latitudes.

[28] 8. That qualitatively discusses the main points of the present statistics. Quantitative discussions, which need detailed modeling for each point, are beyond the scope of the present paper. As a final comment, though a general picture of the occurrence of the ionospheric storms as

Table 2. Ionospheric Storms for Different MP Onset Times at Kokubunji (Dst < −50 nT)[a]

	05–12 LT	13–20 LT	21–04 LT	Total
P-storms	100	57	98	255
PN-storms	28	26	8	62
N-storms	33	34	36	103
NP-storms	5	1	6	12
NS-storms	35	26	31	92
Total	203	143	178	524

[a]See text for P-storms, PN-storms, N-storms, NP-storms and NS-storms.

Table 3. Ionospheric Storms for Different MP Onset Times at Boulder (Dst < −50 nT)[a]

	05–12 LT	13–20 LT	21–04 LT	Total
P-storms	62	28	33	123
PN-storms	28	19	5	52
N-storms	48	96	80	224
NP-storms	3	5	9	17
NS-storms	24	23	22	69
Total	165	170	150	485

[a]See text for P-storms, PN-storms, N-storms, NP-storms and NS-storms.

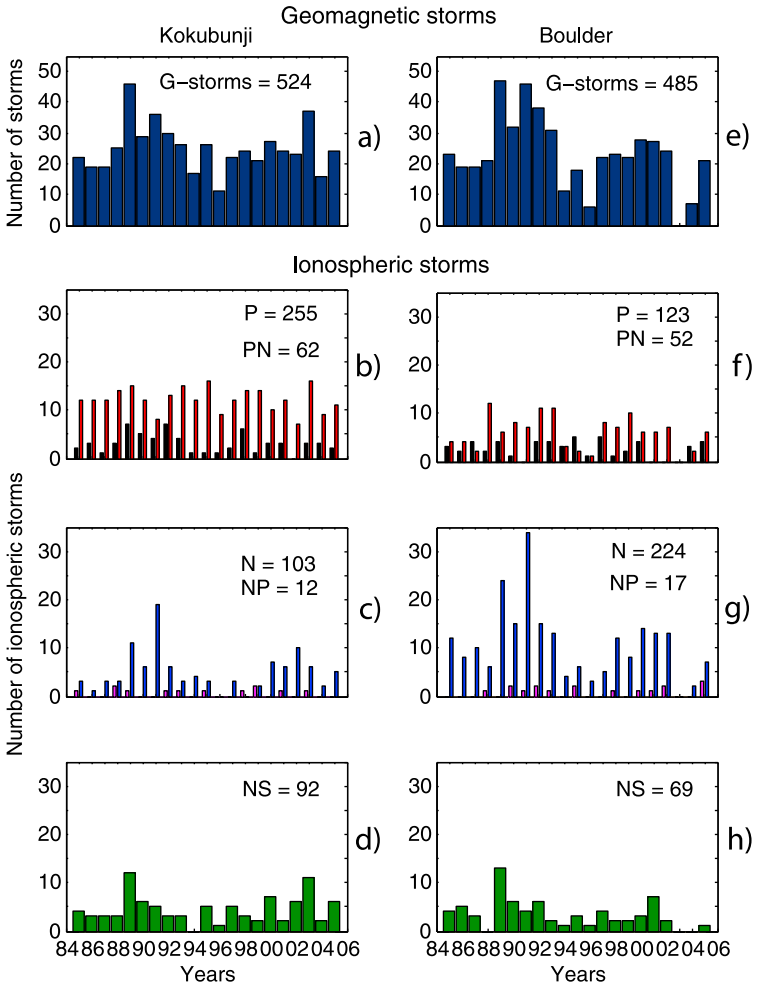

Figure 5. For (left) Kokubunji and (right) Boulder: (a and e) yearly variations of the number of geomagnetic storms for which ionospheric data are available; (b and f) corresponding variations of positive (red) and positive followed by negative (black) ionospheric storms; (c and g) negative (blue) and negative followed by positive (purple) ionospheric storms; and (d and h) non-significant ionospheric storms. Total number of different types of storms is noted.

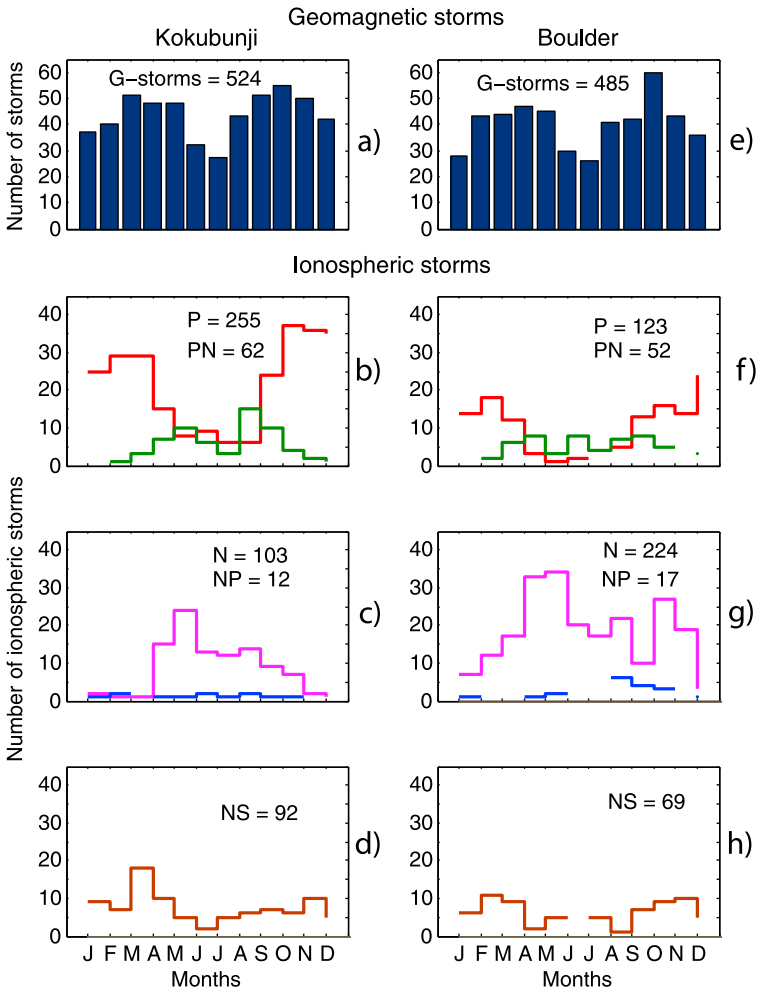

Figure 6. For (left) Kokubunji and (right) Boulder: (a and e) monthly variations of the number of geomagnetic storms for which ionospheric data are available; (b and f) corresponding variations of positive (red) and positive followed by negative (green) ionospheric storms; (c and g) negative (purple) and negative followed by positive (blue) ionospheric storms; and (d and h) non-significant ionospheric storms. Total number of different types of storms is noted.

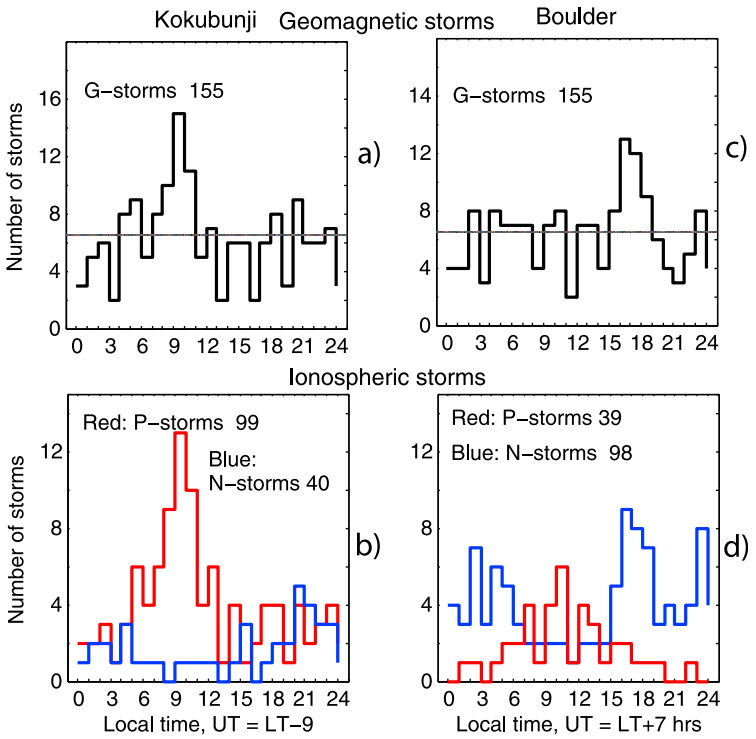

Figure 7. Local time variations of the main phase onset of the number of geomagnetic storms (Dst ≤ −100 nT) for which ionospheric data are available at (a) Kokubunji and (c) Boulder and (b and d) corresponding positive (red) and negative (blue) ionospheric storms. Total number of different types of storms is noted; the horizontal lines (Figures 7a and 7c) represent uniform distributions.

functions of local time, season and location is obtained from the numerous studies for over 50 years, it is not yet possible to say when, where, how (positively or negatively) and how strongly the ionosphere will respond to a given geomagnetic storm. Detailed observations and modeling of the solar wind-magnetosphere-ionosphere-upper atmosphere coupling during solar events such as CMEs (coronal mass ejections) are needed to predict the ionospheric storms that can cause

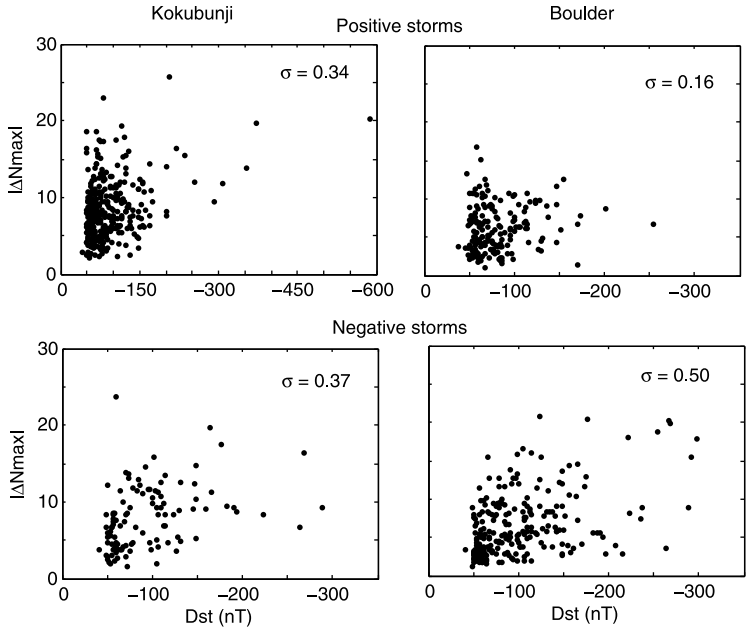

Figure 8. Scatterplot of the strength of (top) positive and (bottom) negative ionospheric storms (magnitude of maximum ΔNmax) at (left) Kokubunji and (right) Boulder against the intensity of geomagnetic storms (minimum Dst).

serious problems in satellite systems, power supply systems, and satellite navigation and communication.

6. Conclusions

[29] The statistics of occurrence of the geomagnetic storms, and ionospheric storms at Kokubunji (26.8°N magnetic latitude) and Boulder (47.4°N) in 1985–2005 when 584 geomagnetic storms occurred reveal some new aspects.

[30] 1. The main phase (MP) onset of the geomagnetic storms shows a preference at around UT midnight especially for major storms, over 100% excess MP onsets compared to a uniform distribution. Though the UT midnight preference is not understood, it is noted that the corresponding noon meridian is in the Pacific sector where the separation between geomagnetic and geographic equators is a minimum and declination angle is nearly constant so that solar wind-magnetosphere coupling and ring current intensification may become more efficient in this than in other longitude sectors.

[31] 2. The number of positive ionospheric storms at Kokubunji (about 250) is more than double that at Boulder as expected from a physical mechanism of the positive storms, which is also supported by a reverse preference for the negative ionospheric storms (about 100 at Kokubunji and 220 at Boulder). (3) The occurrence of the positive storms at both stations also shows a preference for the morning-noon onset of geomagnetic storms as expected. (4) The occurrence of the negative ionospheric storms follows the solar cycle phases (most frequent at solar maximum) better than the occurrence of positive storms, which agrees with the mechanism of the negative storms. (5) The strength of both positive and negative ionospheric storms at both stations shows a weak positive correlation and large scatter with the intensity of the geomagnetic storms, which suggests the large variability of the drivers of the ionospheric storms. (6) In addition to the positive and negative ionospheric storms there are a considerable number of positive storms followed by negative ones (about 65 at Kokubunji and 50 in Boulder), and a small number of negative storms followed by positive ones (about 10 at Kokubunji and 20 at Boulder). (7) There are also a significant number of non-significant ionospheric storms (about 90 at Kokubunji and 70 at Boulder), which seems to suggest the longitude dependencies of the eastward PPEF and energy input at high latitudes.

[32] **Acknowledgments.** N. Balan thanks the Institute of Space Science of National Central University (Taiwan) for providing a Visiting Professor position. The work of STR is supported by JSPS Foundation.

[33] Robert Lysak thanks the reviewers for their assistance in evaluating this paper.

References

Abdu, M. A., et al. (2008), Abnormal evening vertical plasma drift and effects on ESF and EIA over Brazil-South Atlantic sector during the 30 October 2003 superstorm, *J. Geophys. Res.*, *113*, A07313, doi:10.1029/2007JA012844.

Balan, N., and P. B. Rao (1990), Dependence of ionospheric response on the local time of sudden commencement and intensity of storms, *J. Atmos. Terr. Phys.*, *52*, 269–275.

Balan, N., H. Alleyne, S. Walker, H. Reme, I. McCrea, and A. Aylward (2008), Magnetosphere-ionosphere coupling during the CME events of 07–12 November 2004, *J. Atmos. Sol. Terr. Phys.*, *70*, 2101–2111, doi:/10.1016/j.jastp.2008.03.015.

Balan, N., K. Shiokawa, Y. Otsuka, S. Watanabe, and G. J. Bailey (2009), Super plasma fountain and equatorial ionization anomaly during penetration electric field, *J. Geophys. Res.*, *114*, A03310, doi:10.1029/2008JA013768.

Balan, N., K. Shiokawa, Y. Otsuka, T. Kikuchi, D. Vijaya Lekshmi, S. Kawamura, M. Yamamoto, and G. J. Bailey (2010), A physical mechanism of positive ionospheric storms at low and mid latitudes through observations and modeling, *J. Geophys. Res.*, *115*, A02304, doi:10.1029/2009JA014515.

Balan, N., J. Y. Liu, Y. Otsuka, H. Liu, and H. Lühr (2011a), New aspects of thermospheric and ionospheric storms revealed by CHAMP, *J. Geophys. Res.*, *116*, A07305, doi:10.1029/2010JA016399.

Balan, N., et al. (2011b), A statistical study of the response of the dayside equatorial F2 layer to the main phase of intense geomagnetic storms as an indicator of penetration electric field, *J. Geophys. Res.*, *116*, A03323, doi:10.1029/2010JA016001.

Batista, I. S., E. de Paula, M. A. Abdu, N. Trivedi, and M. Greenspan (1991), Ionospheric effects of the March 13, 1989, magnetic storm at low and equatorial latitudes, *J. Geophys. Res.*, *96*, 13,943–13,952.

Blanc, M., and A. D. Richmond (1980), The ionospheric disturbance dynamo, *J. Geophys. Res.*, *85*, 1669–1686.

Buonsanto, M. J. (1999), Ionospheric storm—A review, *Space Sci. Rev.*, *88*, 563–601.

Burns, A. G., T. L. Killeen, W. Deng, G. R. Carignan, and R. G. Roble (1995), Geomagnetic storm effects in the low- to middle-latitude upper thermosphere, *J. Geophys. Res.*, *100*, 14,673–14,691.

Essex, E. A., et al. (1981), A global response of the total electron content of the ionosphere to the magnetic storms of 17 December and 18 June 1972, *J. Atmos. Terr. Phys.*, *43*, 293–306.

Fejer, B. G., J. W. Jensen, T. Kikuchi, M. A. Abdu, and J. L. Chau (2007), Equatorial ionospheric electric fields during the November 2004 magnetic storm, *J. Geophys. Res.*, *112*, A10304, doi:10.1029/2007JA012376.

Foster, J. C. (1993), Storm-time plasma transport at middle and high latitudes, *J. Geophys. Res.*, *98*, 1675–1689.

Fuller-Rowell, T. J., M. V. Codrescu, R. J. Moffett, and S. Quegan (1994), Response of the thermosphere and ionosphere to geomagnetic storms, *J. Geophys. Res.*, *99*, 3893–3914.

Gonzalez, W. D., J. A. Joselyn, Y. Kamide, H. W. Kroehl, G. Rostoker, B. T. Tsurutani, and V. M. Vasyliunas (1994), What is a geomagnetic storm?, *J. Geophys. Res.*, *99*, 5771–5792.

Heelis, R. A., J. J. Sojka, M. David, and R. W. Schunk (2009), Storm time density enhancements in the mid latitude dayside ionosphere, *J. Geophys. Res.*, *114*, A03315, doi:10.1029/2008JA013690.

Huang, C. M., M. Q. Chen, and J. Y. Liu (2010a), Ionospheric positive storm phases at the magnetic equator close to sunset, *J. Geophys. Res.*, *115*, A07315, doi:10.1029/2009JA014936.

Huang, C. S., F. J. Rich, and W. J. Burke (2010b), Storm time electric fields in the equatorial ionosphere near the dusk meridian, *J. Geophys. Res.*, *115*, A08313, doi:10.1029/2009JA015150.

Jones, K. L., and H. Rishbeth (1971), The origin of storm increases of mid-latitude F-layer electron concentration, *J. Atmos. Terr. Phys.*, *33*, 391–401.

Kelley, M. C., M. N. Vlasov, J. C. Foster, and A. J. Coster (2004), A quantitative explanation for the phenomenon known as storm-enhanced density, *Geophys. Res. Lett.*, *31*, L19809, doi:10.1029/2004GL020875.

Kikuchi, T., T. Araki, H. Maeda, and K. Maekawa (1978), Transmission of polar electric fields to the equator, *Nature*, *273*, 650–651.

Lei, J., J. P. Thayer, A. G. Burns, G. Lu, and Y. Deng (2010), Wind and temperature effects on thermosphere mass density response to the November 2004 geomagnetic storm, *J. Geophys. Res.*, *115*, A05303, doi:10.1029/2009JA014754.

Lin, C. H., A. D. Richmond, R. A. Heelis, G. J. Bailey, G. Lu, J. Y. Liu, H. C. Yeh, and S. Y. Su (2005), Theoretical study of the low and mid latitude ionospheric electron density enhancement during the October 2003 storm: Relative importance of the neutral wind and the electric field, *J. Geophys. Res.*, *110*, A12312, doi:10.1029/2005JA011304.

Lu, G., L. P. Goncharenko, A. D. Richmond, R. G. Roble, and N. Aponte (2008), A dayside ionospheric positive storm phase driven by neutral winds, *J. Geophys. Res.*, *113*, A08304, doi:10.1029/2007JA012895.

Mannucci, A. J., B. T. Tsurutani, B. A. Iijima, A. Komjathy, A. Saito, W. D. Gonzalez, F. L. Guarnieri, J. U. Kozyra, and R. Skoug (2005), Dayside global ionospheric response to the major interplanetary events of October 29–30, 2003 "Halloween storms," *Geophys. Res. Lett.*, *32*, L12S02, doi:10.1029/2004GL021467.

Matsushita, S. (1959), A study of the morphology of ionospheric storms, *J. Geophys. Res.*, *64*, 305–321.

Matuura, N. (1972), Theoretical models of ionospheric storms, *Space Sci. Rev.*, *13*, 124–189.

Mayr, H. G., and H. Volland (1973), Magnetic storm characteristics of the thermosphere, *J. Geophys. Res.*, *78*, 2251–2264.
Mendillo, M. (2006), Storms in the ionosphere: Patterns and processes for total electron content, *Rev. Geophys.*, *44*, RG4001, doi:10.1029/2005RG000193.
Mendillo, M., and C. Narvaez (2009), Ionospheric storms at geophysically-equivalent sites—Part 1: Local time patterns for sub-auroral ionospheres, *Ann. Geophys.*, *27*, 1679–1694.
Mendillo, M., and C. Narvaez (2010), Ionospheric storms at geophysically-equivalent sites—Part 2: Local time patterns for sub-auroral ionospheres, *Ann. Geophys.*, *28*, 1449–1462.
Newell, P. T., C.-I. Meng, T. Sotirelis, and K. Liou (2001), Polar ultraviolet imager observations of global aurora power as a function of polar cap size and magnetotail stretching, *J. Geophys. Res.*, *106*, 5895–5905.
Obayashi, T. (1964), *Morphology of Storms in the Ionosphere*, *Rev. Geophys.*, vol. 1, edited by H. Odishaw, pp. 335–366, MIT Press, Cambridge, Mass.
Prölss, G. W. (1995), Ionospheric F region storms, in *Handbook of Atmospheric Electrodynamics*, edited by H. Volland, pp. 195–248, CRC Press, Boca Raton, Fla.
Prölss, G. W., and M. J. Jung (1978), Traveling atmospheric disturbances as a possible explanation for daytime positive storm effects of moderate duration at middle latitudes, *J. Atmos. Terr. Phys.*, *40*, 1351–1354.
Rastogi, R. G. (1977), Geomagnetic storms and electric fields in the equatorial ionosphere, *Nature*, *268*, 422–424.
Rees, D., T. J. Fuller-Rowell, and R. W. Smith (1980), Measurements of high latitude thermospheric winds by rocket and ground-based techniques and their interpretation using a three-dimensional, time-dependent dynamical model, *Planet. Space Sci.*, *28*, 919–932.
Reigber, C., H. Lühr, and P. Schwintzer (2002), CHAMP mission status, *Adv. Space Res.*, *30*, 129–134.
Richmond, A. D., and S. Matsushita (1975), Thermospheric response to a magnetic substorm, *J. Geophys. Res.*, *80*, 2839–2850.
Roble, R. G., R. E. Dickinson, and E. C. Ridley (1982), Global circulation and temperature structures of thermosphere with high-latitude convection, *J. Geophys. Res.*, *87*, 1599–1614.
Russell, C. T., and R. L. McPherron (1973), Semiannual variation of geomagnetic activity, *J. Geophys. Res.*, *78*, 92–108.
Sastri, J. (2002), Penetration electric fields at the nightside dip equator associated with the main impulse of the storm sudden commencement of 8 July 1991, *J. Geophys. Res.*, *107*(A12), 1448, doi:10.1029/2002JA009453.
Sastri, J., N. Jyoti, V. Somayajulu, H. Chandra, and C. Devasia (2000), Ionospheric storm of early November 1993 in the Indian equatorial region, *J. Geophys. Res.*, *105*, 18,443–18,455.
Shepherd, G. G., et al. (1993), WINDII: The WIND imaging interferometer on the Upper Atmosphere Research Satellite, *J. Geophys. Res.*, *98*, 10,725–10,750.
Sreeja, V., S. Ravindran, T. K. Pant, C. V. Devasia, and L. J. Paxton (2009), Equatorial and low latitude ionosphere thermosphere system response to the space weather event of August 2005, *J. Geophys. Res.*, *114*, A12307, doi:10.1029/2009JA014491.
Tulasi Ram, S., S. Su, and C. H. Liu (2009), FORMOSAT-3/COSMIC observations of seasonal and longitudinal variations of equatorial ionization anomaly and its interhemispheric asymmetry during the solar minimum period, *J. Geophys. Res.*, *114*, A06311, doi:10.1029/2008JA013880.
Vijaya Lekshmi, D., N. Balan, V. K. Vaidyan, H. Alleyne, and G. J. Bailey (2007), Response of the ionosphere to super storms, *Adv. Space Res.*, *41*, 548–555, doi:/10.1016/j.asr.2007.08.029.

N. Balan and J. Y. Liu, Institute of Space Science, National Central University, Chung-Li 32054, Taiwan. (b.nanan@sheffield.ac.uk)
S. Tulasi Ram, RISH, Kyoto University, Kyoto 611-0011, Japan.
D. Vijaya Lekshmi, Department of Physics, University of Kerala, Trivandrum 695581, India.